Systemic Fate of the Adipocyte-Derived Factor Adiponectin

Nils Halberg,[1,2] Todd D. Schraw,[1] Zhao V. Wang,[1] Ja-Young Kim,[1] James Yi,[1] Mark P. Hamilton,[1] Kate Luby-Phelps,[3] and Philipp E. Scherer[1,3]

OBJECTIVE—The adipocyte-derived secretory protein adiponectin has been widely studied and shown to have potent insulin-sensitizing, antiapoptotic, and anti-inflammatory properties. While its biosynthesis is well understood, its fate, once in circulation, is less well established.

RESEARCH DESIGN AND METHODS—Here, we examine the half-life of adiponectin in circulation by tracking fluorescently labeled recombinant adiponectin in the circulation, following it to its final destination in the hepatocyte.

RESULTS—Despite its abundant presence in plasma, adiponectin is cleared rapidly with a half-life of ~75 min. A more bioactive version carrying a mutation at cysteine 39 is cleared within minutes. Even though steady-state levels of adiponectin differ between male and female mice, we failed to detect any differences in clearance rates, suggesting that differences in plasma are mostly due to differential production rates. In a metabolically challenged state (high-fat diet exposure or in an *ob/ob* background), adiponectin levels are reduced in plasma and clearance is significantly prolonged, reflecting a dramatic drop in adiponectin production levels.

CONCLUSIONS—Combined, these results show a surprisingly rapid turnover of adiponectin with multiple fat pads contributing to the plasma levels of adiponectin and clearance mediated primarily by the liver. It is surprising that despite high-level production and rapid clearance, plasma levels of adiponectin remain remarkably constant. ***Diabetes*** **58:1961–1970, 2009**

Adiponectin is a relatively abundant protein secreted from adipocytes circulating in the micrograms per milliliter range. It acutely lowers blood glucose levels through suppression of hepatic glucose levels and chronically has potent insulin-sensitizing effects through reduction of hepatic lipids (1–3). Various disease states are associated with lower plasma adiponectin levels. Specifically, type 2 diabetic subjects and patients with early-stage cardiovascular disease have lower levels of adiponectin (4,5).

From the [1]Touchstone Diabetes Center, Department of Internal Medicine, University of Texas Southwestern Medical Center, Dallas, Texas; the [2]Department of Biomedical Sciences, Faculty of Health Science, University of Copenhagen, Copenhagen, Denmark; and the [3]Department of Cell Biology, University of Texas Southwestern Medical Center, Dallas, Texas.
Corresponding author: Philipp E. Scherer, philipp.Scherer@utsouthwestern.edu.
Received 17 December 2008 and accepted 8 June 2009.
Published ahead of print at http://diabetes.diabetesjournals.org on 6 July 2009. DOI: 10.2337/db08-1750.

Adiponectin circulates in three different forms: high molecular weight (HMW) (18–36 mer), low molecular weight (LMW) (hexamer), and a trimeric form. Levels of the HMW form are tightly connected to insulin sensitivity (6). The relevance of the hexameric and trimeric forms has not yet been systematically addressed. Stable higher-order complex formation requires the presence of disulfide bond formation at position 39. Recombinant versions of adiponectin carrying a conversion of cysteine 39 to an alanine display much more potent glucose-lowering effects than wild-type protein (7). This suggests that a reduction step at the level of the target organ may play an important role in the activation of the protein into a bioactive form. Direct evidence for such a step is, however, lacking to date. The three monomers constituting the trimer form of adiponectin are held together via a strong hydrophobic trimer interface in the globular head as well as a highly dithiotreitol (DTT)-resistant intratrimer disulfide bond. Hence, converting cysteine 39 to an alanine results in predominantly trimeric isoforms, which differ from the native trimer form by the intratrimer dilsufide bond.

Once secreted, adiponectin may exert its effects through binding to a set of receptors, such as the adipoR1 and adipoR2 and/or T-Cadherin (8,9). Although activation of AMP-activated kinases as well as peroxisome proliferators–activated receptor α are postulated to play a role in mediating the adiponectin signal in liver and muscle, the direct signaling pathways remain somewhat controversial. In addition, the relevance of the adipoR1 and adipoR2 has been questioned in several publications (10,11).

As with any protein in circulation, steady-state levels are governed by the rate of release and the clearance rate of the protein. Despite a wealth of data on transcriptional and posttranslational regulation of adiponectin in the secretory pathway, the clearance of adiponectin has not been studied. Here, we take advantage of a dye-labeled, mammalian-produced recombinant adiponectin preparation that fluoresces in the near-infrared range and use these preparations to follow the fate of adiponectin in vivo.

RESEARCH DESIGN AND METHODS

Mice (FVB) were maintained on a 12-h dark/light cycle and fed a normal diet. All animals were 8–10 weeks old at the time of the experiments. For clearance studies, wild-type FVB, adiponectin-null FVB, and FVB *ob/ob* mice were bred in-house in our animal facility. Pregnant mice were used on day 18 after conception. Characterization and description of the mice overexpressing adiponectin from the liver is currently in progress (K.D. and P.E.S., unpublished data). The high-fat diet consisted of 60 E% from fat (Research Diets, New Brunswick, NJ). The institutional animal care and use committee of the University of Texas Southwestern Medical Center and the Albert Einstein College of Medicine approved all animal experimental protocols. The IRDye800CW and 700CW infrared N-hydroxisuccinimide ester dyes were purchased from Licor Biotechnology (Lincoln, NE). Protease inhibitor cocktail was obtained from Calbiochem. Sterile PBS was purchased from EMD Chemicals.

Protein production and labeling. Wild-type and cysteine 39 adiponectin were produced as previously described (7,12). To isolate HMW, LMW, and

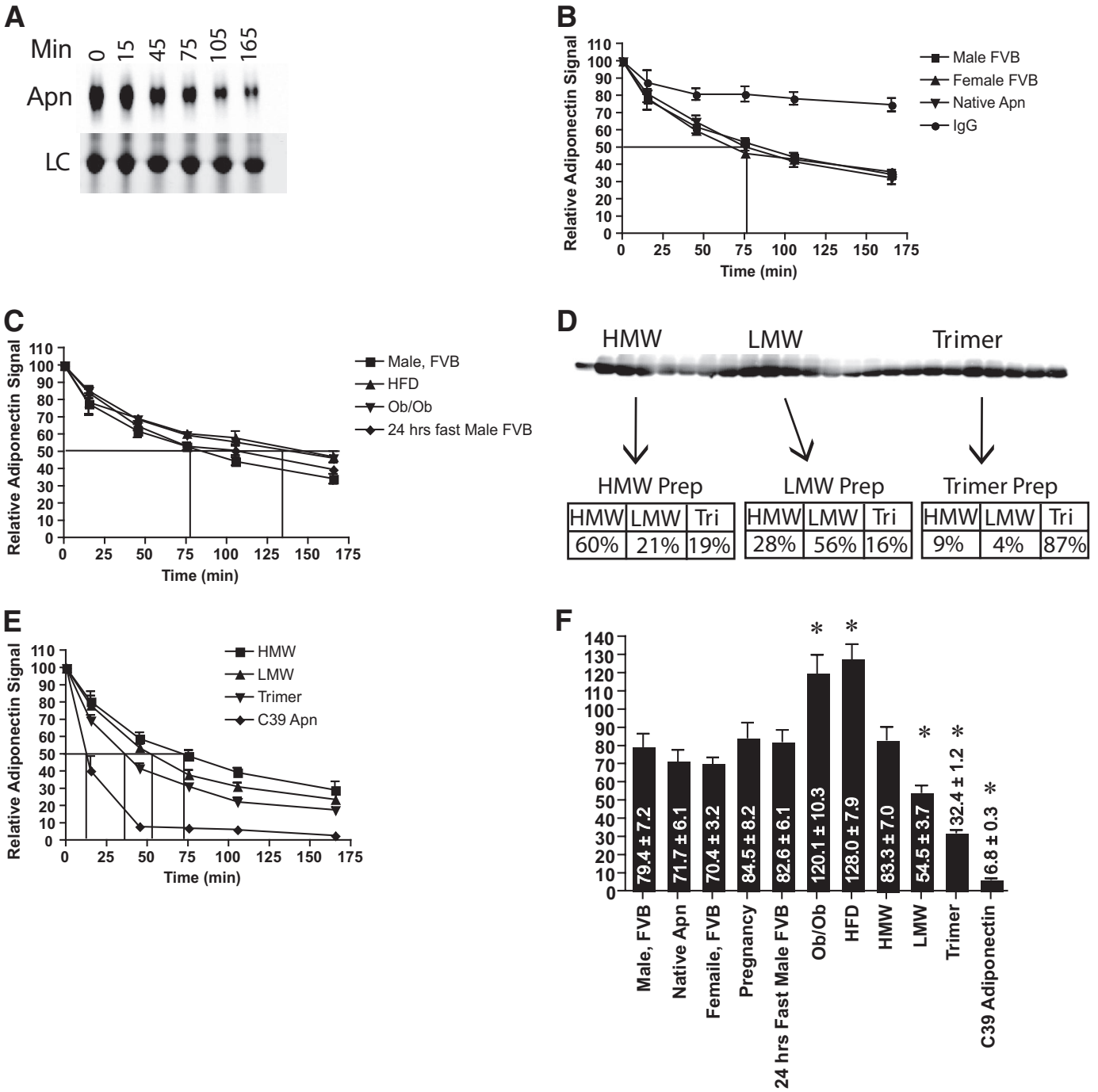

FIG. 1. Adiponectin clearance. *A*: *Upper panel* shows the fluorescent signal from the injected labeled adiponectin gel scan of 1.5 µl serum separated on SDS-PAGE over time. The *lower panel* shows the same gel after a Coomassie stain for loading control. Apn, Adiponectin; LC, immunoglobulin light chain. *B*: Clearance curve for wild-type adiponectin in male and female FVB mice as well as native adiponectin and IgG. The clearance of native adiponectin was determined by injecting wild-type serum into adiponectin-null mice. *C*: Clearance curves for male FVB mice fed a normal as well as high-fat diet, male *ob/ob* FVB mice, and male FVB mice fasted 24 h. *D*: To isolate the three forms of adiponectin, recombinant adiponectin containing all three forms (*upper panel*) were subjected to gel filtration to create elutions containing the individual isoforms. The *lower panel* shows a subsequent analysis of the complex distribution of the isolated fractions. *E*: The clearance curve of isolated HMW, LMW, trimer, and cysteine 39 adiponectin in male FVB mice. *F*: The calculated half-life for wild-type adiponectin in male, female, pregnant female, 24-h–fasted male, *ob/ob* mice, high-fat diet–fed mice, isolated HMW, isolated LMW, isolated trimer, and for the cysteine 39 adiponectin in male mice. $n = 4$ per group. *$P < 0.05$ vs. clearance rate of male wild-type FVB mice.

trimer isoforms, recombinant adiponectin was separated by fast protein liquid chromatography and 24 fractions were collected. Adiponectin levels in the different fractions were then analyzed by Western blotting, and the fractions containing the individual complexes were collected and concentrated to a final protein concentration of 1 mg/ml. Validation of the enrichment of the different isoforms showed that we were able to isolate fractions highly enriched in the various isoforms (Fig. 1*D*). Mouse IgGs were purchased from Sigma Aldrich. Wild-type and cysteine 39 adiponectin, HMW, LMW, and trimer were derivatized with the IRDye 800CW, and IgGs were labeled with IRDye 700CW at a dye:protein 1:1 molar ratio, according to the manufacturer's instructions.

Analysis for half-life determinations. The circulating half-life of adiponectin was determined in the following settings: 8-week-old male and female FVB mice, in females pregnant at day 18, in males fasted for 48 h, in 8-week-old *ob/ob* male FVB mice, and in male FVB mice fed a high-fat diet for 6 weeks. In addition, the circulating half-life of HMW, LMW, trimer, and cysteine 39

adiponectin were determined in 8-week-old male FVB mice. We and others have previously determined adiponectin levels under these various conditions in Combs et al. 2003 (13), Berg et al. 2001 (1), and Haluzik et al. 2004 (14). For all conditions, the clearance was determined by injecting 0.05 μg labeled adiponectin/g body wt into the tail vein and by collecting blood samples at the indicated time points in heparinized capillary tubes. A total of 1.5 μl plasma was subsequently mixed with 19 μl TBS and 5 μl 5 × Laemmli buffer. After separation on a 10% Bis-Tris gel (Invitrogen, Carlsbad, CA), the labeled proteins were directly visualized in the gel on the Licor Odyssey infrared imaging system in the 700- and 800-nm channels, without any prior staining techniques or transfers. Following scanning, the gel was stained with Commassie Blue stain, and the IgG light-chain band was quantified as loading control. The 32-kDa adiponectin band obtained from the gel scans and the 25-kDa IgG light-chain band from the Coommassie stain were quantified with Odyssey version 2.1 software.

In a final set of experiments, the clearance of endogenous adiponectin was studied by injecting 200 μl serum from wild-type mice into 8-week-old adiponectin-null mice. The levels of circulating adiponectin at the various time points in the adiponectin-null mice were determined by enzyme-linked immunosorbent assay (Millipore). The circulating half-life of adiponectin was defined as the time it took to remove 50% of the injected material from circulation.

Analysis of mouse adiponectin complexes. Analysis of the adiponectin complex distribution was performed as described in Schraw et al. (12) using a rabbit polyclonal anti-mouse adiponectin primary antibody.

Scanning of mice in vivo. Prior to injection of the labeled material, chest and abdominal hair was removed with Nair hair remover (Church & Dwight). All scans were performed under anesthesia (Aerrane, Baxter, IL) using an EZ-2000 Microflex small-animal anesthesia system (EZ Systems, Palmer, PA). Once under full anesthesia, the mice were transferred to an Odyssey Infrared Scanner (Li-Cor Biosciences, Lincoln, NE) with an Odyssey mousePOD connected to the anesthesia apparatus. The full-body scans were performed with a resolution of 169 μm, a focal plane lifted 4 mm, and the fluorescence was measured in the 700- and 800-nm channels. Following the initial prescan, the labeled material was injected into the tail vein. Wild-type and cysteine 39 adiponectin and IgGs were given at 0.05 μg/g body wt in a total volume of 200 μl. For the control experiments, wild-type adiponectin was denatured and reduced by boiling for 15 min with the presence of 1% SDS and 1 mmol/l DTT in a total volume of 50 μl. At the indicated time points, the mice were scanned and the liver signals were quantified using the Odyssey version 2.1 software.

Organ analysis. To remove residual labeled material in the blood stream, the mice were perfused (3.6 ml/min) with 20 ml PBS by entry into the left ventricle and exit through the right atrium. The target organs were excised and scanned on the Odyssey Infrared Scanner in the 800-nm channel. Following the scan, tissues were snap frozen. To further process samples, they were homogenized in TNET buffer (50 mmol/l Tris, pH 7.5; 150 mmol/l NaCl; 5 mmol/l EDTA; and 1% Triton X-100) with protease inhibitors and centrifuged at 14,000 rpm for 15 min at 4°C. The protein concentration of the supernatants was measured with the bicinchoninic assay (Pierce), and 20 μl were spotted directly on to a nitrocellulose membrane. The signals on the membranes were directly quantified (without any washing) with the Odyssey Infrared Scanner.

Microscopy and immunofluorescence. To visualize exogenously administered adiponectin, 8-week-old adiponectin-null mice were administered 0.5 μg/g body wt wild-type and cysteine 39 adiponectin or PBS. After 2 h and 20 min, the mice were perfusion fixed with 10% formalin. For detection of endogenous adiponectin, 8-week-old adiponectin-null and wild-type mice were perfusion fixed in 10% formalin. In both experiments, the liver, kidney, spleen, and gastrocnemius muscle were excised and processed for histology. Tissue sections were decorated with an antibody targeting the NH_2-terminal region of adiponectin, anti-K8/18, and 4′,6-diamidino-2-phenylindole. Fluorescence was detected using the Leica TCS SP5 confocal microscope. Images were processed using ImageJ (Wayne Rasband, National Institutes of Health). The same set of image processing steps was applied to both the control and the experimental images.

Statistics. The results are shown as means ± SE. All statistical analysis was performed in SigmaStat 2.03 (SysStat Software, Point Richmont, CA). Differences in Fig. 1*B* were determined by the two-way ANOVA for repeated measures. For comparison between two independent groups, the Student's *t* test was used. Significance was as accepted at $P < 0.05$.

RESULTS

Rapid clearance of adiponectin from circulation. Adiponectin was recombinantly produced in 293-T cells as previously described (15). This preparation was subsequently derivatized with a N-hydroxisuccinimide–IRDye 800CW such that each trimer was labeled with ~1 dye molecule. The derivatized molecule retained its multimeric conformation (online appendix Fig. 1 [available at http://diabetes.diabetesjournals.org/cgi/content/full/db08-1750/DC1) and maintained its bioactivity as judged by its ability to induce a glucose-lowering effect in vivo if injected at 0.5 μg/g body wt (data not shown). To determine the clearance rate for adiponectin during different physiological as well as pathophysiological conditions, we injected these preparations intravenously into mice and frequently sampled plasma levels over the next 3 h. Figure 1*A* (*upper panel*) shows the fluorescence derived from the labeled adiponectin after separation on SDS-PAGE containing plasma from mice injected with labeled adiponectin. The *lower panel* shows the 25-kDa IgG light-chain band of a subsequent Coommassie stain of the same gel, serving as a loading control.

While females tend to have significantly higher levels of adiponectin in circulation, wild-type adiponectin clears plasma with a rate of ~75 min in both male and female FVB mice (Fig. 1*B* and *F*). To validate that our labeled recombinant adiponectin behaves similar to native adiponectin in circulation, we injected 200 μl serum from wild-type mice into adiponectin-null mice and measured clearance of adiponectin levels by enzyme-linked immunosorbent assay over the next 3 h (Fig. 1*B* and *F*). No differences could be observed between the endogenous ("native") adiponectin and the recombinant, purified adiponectin.

Next, we wanted to know whether conditions characterized by altered adiponectin levels also had differences in clearance rates. We have previously shown that long-term fasting causes adiponectin levels to increase significantly. Comparing clearance rates between ad libitum–fed mice and mice fasted for 24 h did not reveal any differences at the level of clearance (Fig. 1*C* and *F*). We have also shown that during pregnancy, adiponectin levels drop significantly, in line with the decreased systemic insulin sensitivity in the mothers (16). However, clearance rates between female control mice and a cohort of pregnant females did however not reveal any differences, suggesting that a reduction of adiponectin production is the major driving force behind the systemic reduction (Fig. 1*F*). Even more striking is our observation that the half-life of adiponectin is significantly extended in *ob/ob* mice or in wild-type mice exposed to a high-fat diet compared with wild-type controls fed a standard diet (Fig. 1*E* and *F*). The decreased plasma levels found under these conditions are therefore primarily due to the reduced production rate in these animals.

The HMW form of adiponectin has been shown to correlate better to insulin sensitivity than total levels (6). We therefore wondered if the clearance of the individual adiponectin complexes differed in regards to clearance rate. The three isoforms were isolated by gel filtration of recombinant adiponectin and labeled at the ratio of one dye per trimeric subunit (Fig. 1*D* and *F*). Interestingly, the half-life did in fact diverge between HMW, LMW, and the trimer isoform, such that HMW has the slowest clearance (83.3 ± 7 min), followed by LMW (54.5 ± 3.7 min) and trimer (32.4 ± 1.2 min). Surprisingly, the much more bioactive cysteine 39 mutant protein cleared the system with a half-life of <10 min (6.8 ± 0.3 min).

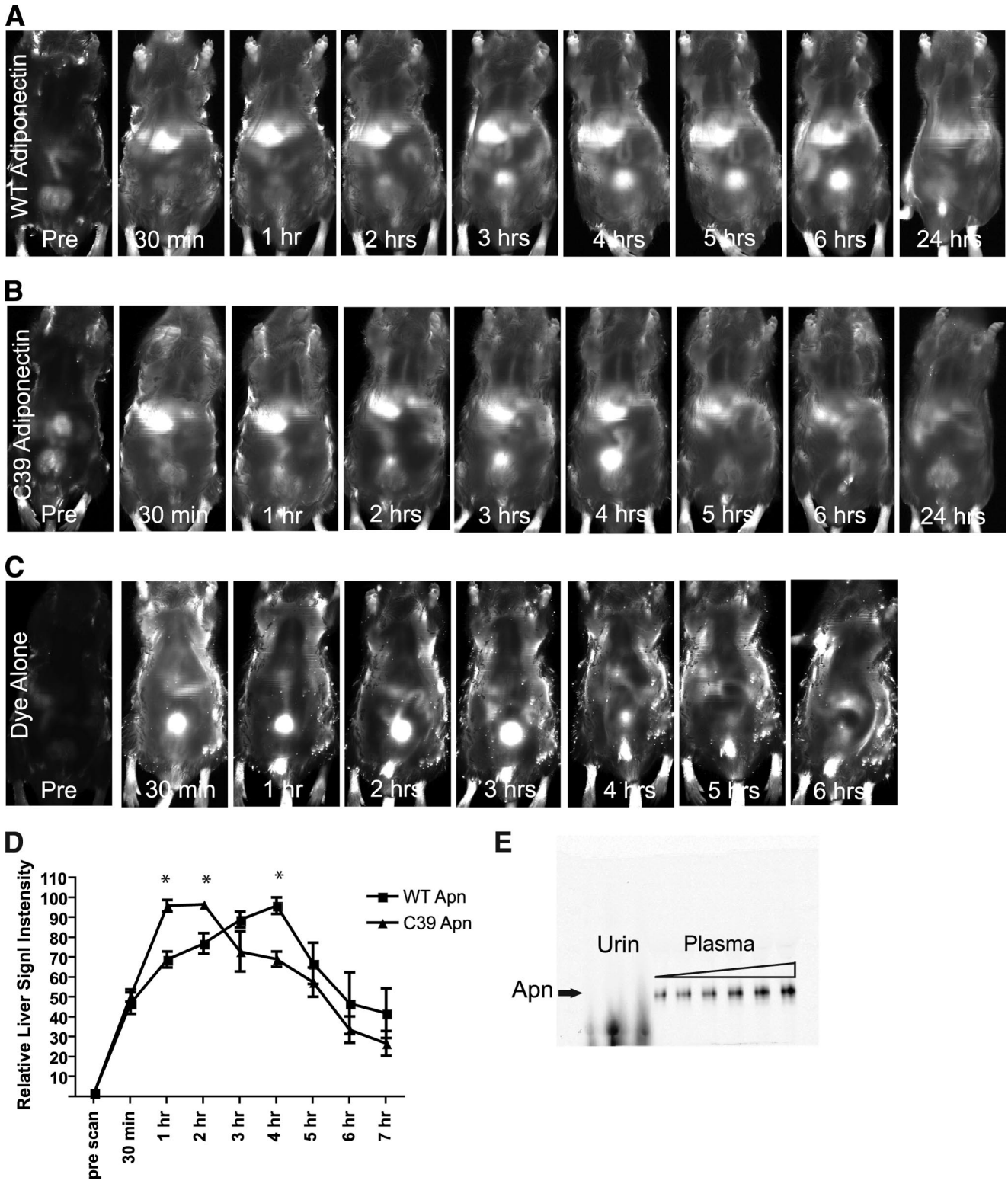

FIG. 2. Whole-body imaging of injected adiponectin. Visualization of injected labeled mammalian produced wild-type adiponectin (*A*), cysteine 39 adiponectin (*B*), and quenched IRDye800 without conjugation to protein by the Licor Infrared Scanner (*C*). Wild-type (WT) and cysteine 39 adiponectin were injected (0.05 μg/g body wt) and the mice scanned 30 min, 1, 2, 3, 4, 5, 6, and 24 h postinjection. *D*: The liver signals from *A* and *B* were quantified and plotted over time. *$P < 0.05$ between the wild-type and cysteine 39 protein. $n = 4$ for each set of injections. *E*: SDS-PAGE analysis of labeled adiponectin in the urin and in the plasma.

The liver is the primary clearance site for adiponectin. Preparations of the wild-type protein and the cysteine 39 mutant were injected intravenously into wild-type mice, and the distribution of the labeled protein was followed longitudinally in real time using a Licor Infrared detector unit highly sensitive to emission wavelengths in the infrared range. Detection at these very long wavelengths has the advantage that there are very low levels of autofluo-

rescence caused by tissues. Also, these wavelengths are associated with deeper penetration into the tissues compared with wavelengths within the visible spectrum.

Upon injection, both the wild-type (Fig. 2*A*) and cysteine 39 mutant proteins (Fig. 2*B*) partition to the liver. In contrast, the injection of quenched dye alone causes clearance through the kidney and elimination from the system through urine as judged by the bright appearance of the bladder (Fig. 2*C*). In line with the differential clearance rates, the cysteine 39 mutant accumulates with considerably faster kinetics than wild-type protein. A quantification of the total signal in the liver and its changes over time are shown in Fig. 2*D*. This highlights the fact that the signal for the cysteine 39 mutant peaks as early as 30 min, whereas the signal for the wild-type protein takes up to 4 h to accumulate the highest signal intensity. Both proteins seem to get degraded, and the fluorescent label can ultimately be found in the bladder as well. At this stage, however, the protein is no longer full length, and labeled adiponectin can only be detected as a broad heterogeneous smear when urine samples are separated on SDS-PAGE (Fig. 2*E*). Although the different kinetics of liver signal between the wild-type and cysteine 39 adiponectin are in it self highly suggestive of a specific signal and not just a fluid-phase uptake phenomenon, we performed two additional control experiments. First, we wanted to test the outcome if we disrupt the original structure of the recombinant protein by boiling the preparation in the presence of 1% SDS and 1 mmol/l DTT. Even though some of this material may partially refold in vivo, this preparation accumulated to a different extent and with completely different kinetics in the liver and displayed a clearance rate comparable to that of the cysteine 39 adiponectin (online appendix Figs. 2 and 5). In addition, we wanted to compete the liver binding of labeled adiponectin with increased levels of endogenous adiponectin. For this purpose, we used a transgenic mouse model engineered to express adiponectin from the liver under the control of the transthyretin promoter. These mice have a fourfold increase in circulating adiponectin compared with wild-type mice (K.D., P.E.S., unpublished observations). Similar to the denatured material, the injected adiponectin bound the liver with radically different kinetics (online appendix Figs. 3 and 4). Importantly, in both cases we set the maximal level to 100% to display the kinetics of clearance in relative terms. It is difficult to assess the absolute levels of tissue accumulation between different injections in quantitative terms, but the signal intensity in the liver was distinctly lower with both denatured adiponectin as well as in the overexpressing mice relative to injection of native protein into wild-type mice.

Liver and kidney accumulate exogenously administered adiponectin most efficiently. The detection of labeled adiponectin in the intact animal offers the advantage of monitoring the distribution of the protein in real time. While powerful from a global perspective, this suffers from the inherent disadvantage that some organs may appear selectively more intense due to the closer proximity to the detection unit. To overcome this bias, organs were excised upon injection of wild type (4 h) and cysteine 39 mutant (1.5 h) post injection. Organs were harvested and protein lysates were prepared and quantified by dot-blot analysis (Fig. 3*A*). As expected from the whole-body images, the liver and kidneys are responsible for the major adiponectin signal intensity. When the protein lysates were separated on SDS-PAGE, the adiponectin could

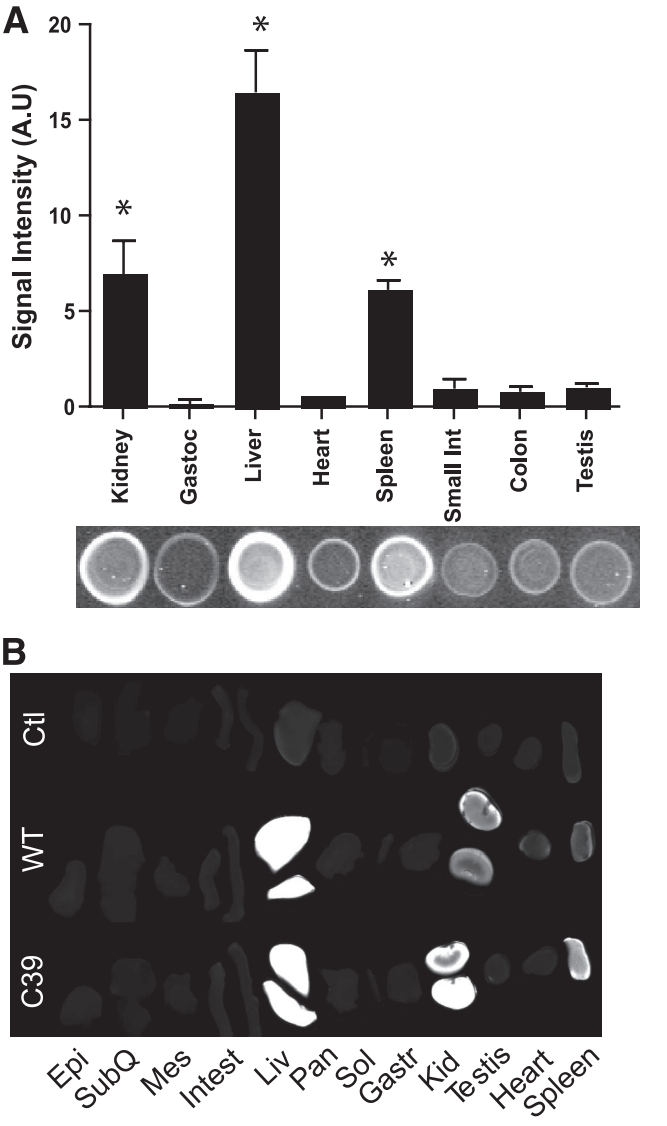

FIG. 3. Adiponectin target organs. *A*: Dot-blot analysis of injected wild-type (WT) adiponectin in different organ lysates 4 h postinjection. Bar graph shows the signal intensity and below a representative dot blot. *B*: Representative direct infrared scanning of the full organs 4 h postinjection. Epi, epididymal white adipose tissue; Gast, gastrocnemius muscle; Kid, kidney; Liv, liver; Mes, mesenteric white adipose tissue; Pan, pancreas; Sol, soleus muscle; SubQ, subcutaneous white adipose tissue. *n* = 4.

only be visualized as a smear in all cases (data not shown), indicating a rapid degradation once the molecule is taken up inside the cell. Surprisingly, we also found a significant signal in the spleen, whereas we detected only very low signal in gastrocnemius, heart, small intestine, colon, pancreas, white adipose tissue, or testis. These observations were confirmed by scanning whole organs directly on the infrared scanner (Fig. 3*B*). Even though we saw a relatively high intensity signal in spleen, we were unable to demonstrate that this is a specific signal. Upon analysis of the spleens from mice injected with boiled and reduced adiponectin, we observed the same signal (data not shown), suggesting that the signal in the spleen is unspecific. Importantly however, even though the organs we examined displayed relatively low or no specific signal for adiponectin, we cannot rule out that a small subset of cells within a given tissue bind and take up adiponectin avidly. Our goal here is to determine whole-organ

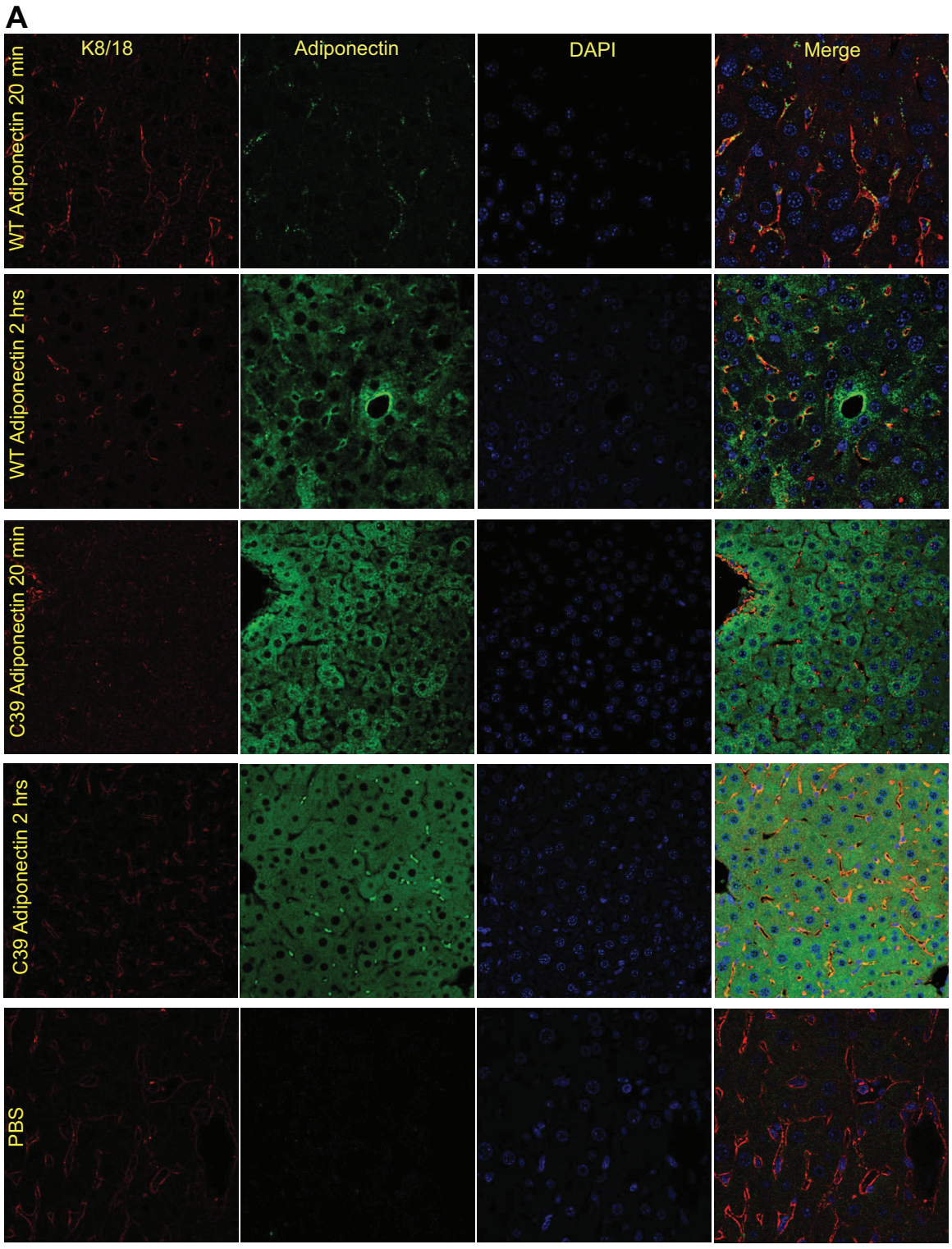

FIG. 4. Visualization of exogenously administered adiponectin in the liver and kidney. *A*: Wild-type (WT) and cysteine 39 adiponectin were injected (0.5 μg/g body wt) into adiponectin-null mice and the liver processed for histology. The exogenous adiponectin was next visualized in the liver using an antiadiponectin antibody 20 min and 2 h postintravenous injections. As a control, PBS was injected without any adiponectin. K8/18 was used as an endothelial marker, and DAPI was used to visualize the nuclei. *B*: Adiponectin and DAPI stain in the kidney 20 min and 2 h after intravenous injection of adiponectin into adiponectin-null mice. (A high-quality digital representation of this figure is available in the online issue.)

contribution to clearance. Low levels of signal in an organ should not be taken to rule out uptake of adiponectin by a small subset of cells, rather it indicates that a particular tissue is not a major contributor to clearance as a whole.

Clearance of the adiponectin signal at the cellular level. Given the high intensity of signal in the liver, we wondered whether we could develop an imaging method that would enable us to monitor the uptake of injected adiponectin into hepatocytes. To that end, we injected

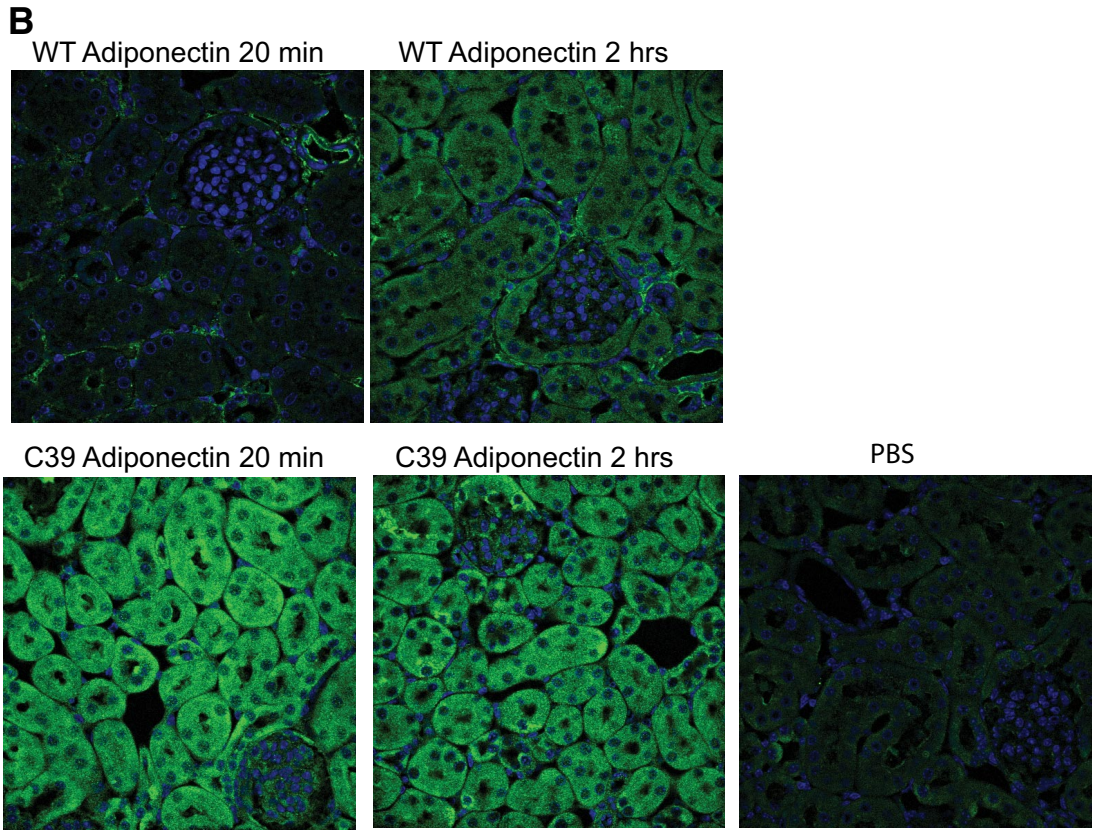

FIG. 4. Continued.

nonlabeled wild-type and cysteine 39 adiponectin (0.5 μg/g body wt) intravenously into adiponectin-null mice and sampled livers at 20 min and 2 h. In line with the more rapid kinetics of the cysteine 39 mutation, the adiponectin signal in the hepatocyte was prevalent at the early 20-min time point, whereas the wild-type adiponectin signal at this stage was located in the surrounding microvessels as evident by a colocalization with K8/18 (Fig. 4*A*). Two hours after injection, adiponectin can be seen intracellularly in the hepatocytes for both wild-type and cysteine 39 adiponectin (Fig. 4*A*). As these images were obtained by immunofluorescence, we do not known whether the signal arises from full-length or degraded adiponectin. As for kidney, wild-type adiponectin could only be detected weakly in the kidney sections 20 min after injection, whereas the more active cysteine 39–mutated adiponectin was abundantly apparent intracellularly at this time point as well. After 2 h, the cysteine 39 signal in the kidney was already markedly decreased as suspected by the short half-life. Levels of wild-type adiponectin, however, were increased compared with 20 min (Fig. 4*B*). Notably, the adiponectin detected in the kidney is mostly in the tubules with more limited signal in the glomeruli and appears to be mostly intracellular. No signal could be detected in the spleen or in gastrocnemius muscle (data not shown). The lack of signal in the spleen confirms the nonspecific nature of the signal in this tissue, as discussed above.

Endogenous adiponectin. To further validate that the exogenous material behaved comparably to endogenous adiponectin, we visualized endogenous adiponectin in liver sections from wild-type and adiponectin-null mice. This, of course, represents a steady-state level of adiponectin as compared with the bolus injection described above. As seen for the exogenous adiponectin, endogenous adiponectin can be located to larger vessels in the liver (Fig. 5*A*), which is in accordance with previously published data (17). In addition, we were able to detect adiponectin surrounding the individual hepatocytes with a distinct plasma membrane stain (Fig. 5*A*). Intracellular adiponectin was also detected, although at much lower frequency and much weaker than that observed with injected adiponectin, confirming that in the steady-state adiponectin (or at least the epitope that we use for visualization with our antibodies) is degraded rapidly. As with the liver, we were able to detect adiponectin signal in the blood vessels of the kidney (Fig. 5*B*). However, we did not reproducibly pick up intracellular signal. Interestingly, when we probed the gastrocnemius muscle for endogenous adiponectin, we detected a sarcolemal signal (Fig. 5*B*). This was not seen with the exogenous adiponectin. There is still only weak evidence available arguing for an in vivo action of adiponectin on muscle. It remains unclear whether adiponectin plays a physiological role in muscle and what the sarcolemmal signal indicates.

DISCUSSION

To our knowledge, this is the first study that addresses the in vivo fate of adiponectin and determines its half-life in circulation under both physiological and pathophysiological conditions. We have found that adiponectin circulates with a half-life of ~75 min. This clearance state is relatively stable and shows no difference between the sexes, with long-term fasting, or during pregnancy (all situations known to alter the circulating levels of adiponectin). That said, however, both genetically (*ob/ob* mice) and diet-

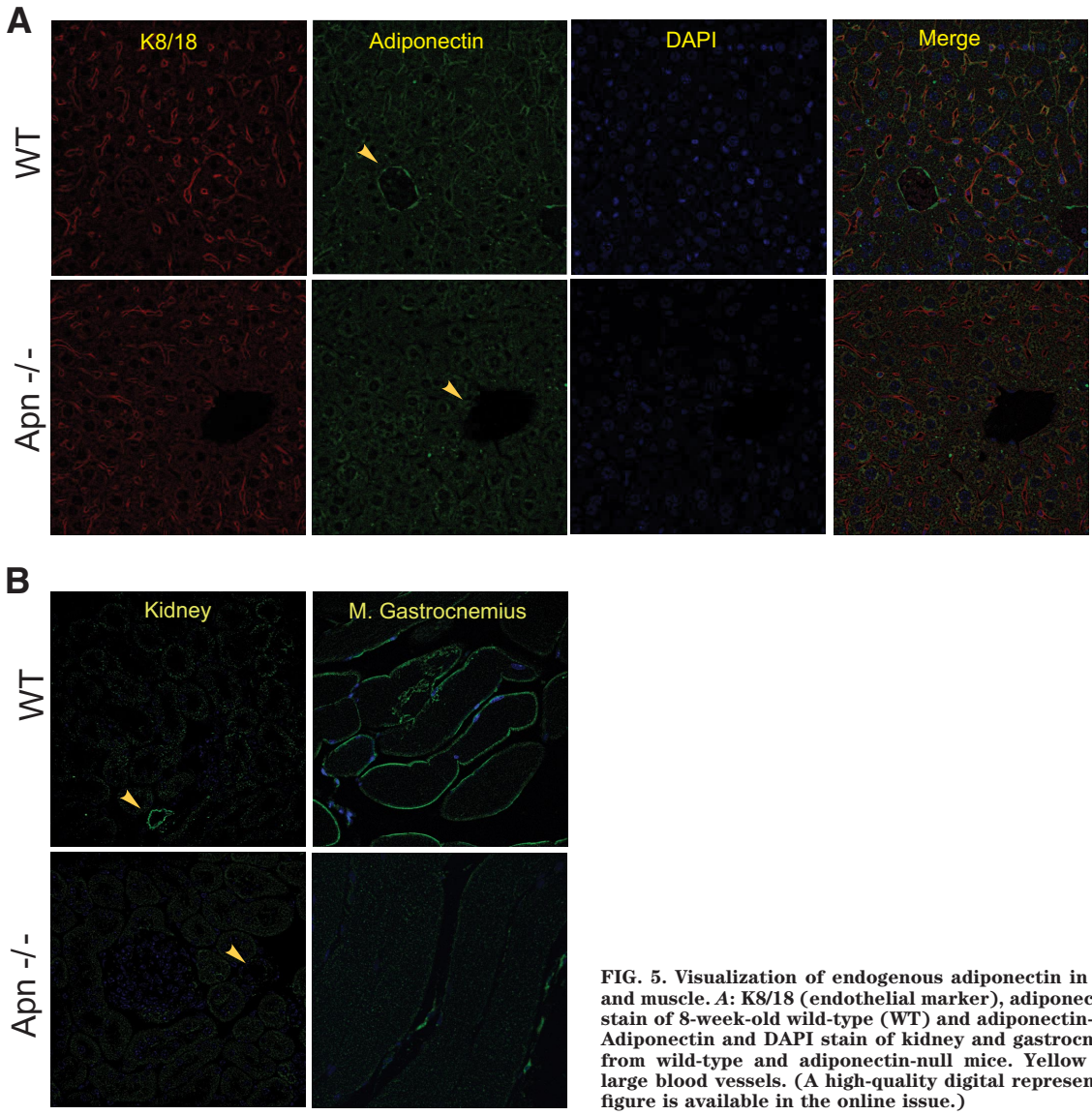

FIG. 5. Visualization of endogenous adiponectin in liver, kidney, and muscle. *A*: K8/18 (endothelial marker), adiponectin, and DAPI stain of 8-week-old wild-type (WT) and adiponectin-null livers. *B*: Adiponectin and DAPI stain of kidney and gastrocnemius muscle from wild-type and adiponectin-null mice. Yellow arrows show large blood vessels. (A high-quality digital representation of this figure is available in the online issue.)

induced obesity resulted in slower clearance rates of adiponectin. Thus, the lower adiponectin levels observed under these conditions must be a result of diminished secretion rather than an increased clearance.

At this stage, there is very limited evidence to whether the three different adiponectin complexes have similar functions or work in concert with each other. The fact that HMW adiponectin levels are more tightly correlated with insulin sensitivity than total adiponectin suggests that there might be differences. Here, we show that HMW, LMW, and trimer adiponectin are cleared differentially, in such that HMW is cleared slowest ($T_{1/2}$ ~85 min) and trimer fastest ($T_{1/2}$ ~32 min). At this stage, we can only speculate as to why the HMW form is cleared more slowly than the other two isoforms. The HMW form may serve as a storage compartment for trimeric subunits that get locally generated upon reduction of the HMW form. Alternatively, exit of the HMW form from circulation may be slowed down due to its size. The time in circulation for trimeric adiponectin can be even further reduced to 10 min by mutating cysteine 39 to alanine. We do not believe that this shortened half-life is a reflection of an unfolded or generally unstable recombinant protein for several reasons. First, this recombinant protein is highly bioactive. Second, we have generated transgenic mice that overexpress this mutant in adipocytes. While the synthesis and release of this protein occurs at levels comparable to wild-type protein, the steady-state levels of the mutant are <1% of wild-type levels, consistent with a very short half-life of this protein in circulation (K.D., T.S., P.E.S., unpublished observations). The cysteine 39 mutant adiponectin is physiologically more active as determined by its ability to lower glucose. This implies that the intratrimer disulfide bond (the only difference between wild-type trimer and cysteine 39 mutant) plays a key role. The intratrimeric disulphide bond may maintain the wild-type protein in a "spring-loaded" configuration that conveys a conformational change throughout the protein upon reduction.

It is interesting to note that the potently bioactive cysteine 39 mutant is also the form with the fastest clearance. Combined with the delayed clearance of adiponectin in the high-fat diet and *ob/ob* models, this suggests that rapid clearance goes hand in hand with high bioavailability and activity, whereas delayed clearance is an indicator of metabolic dysfunction. Importantly, however, these are only correlations, and we are focusing here

at clearance only and do not want to imply that clearance equates bioactivity under all circumstances.

These differential effects on clearance of adiponectin raise the important question as to how the clearance of this protein is mediated. This remains a vastly unexplored area. Like adiponectin, insulin has a profound effect on the liver. After binding to the insulin receptor on the hepatocyte, the receptor-protein complex gets internalized into the endosome where the insulin-degrading enzyme breaks down the insulin (18). While insulin has a much shorter half-life than adiponectin, it may be possible that adiponectin (similar to insulin) is extracted every time it passes through the liver. The detection methods used to date are not sensitive enough to measure a gradient across the splanchnic bed, but a combination of more robust assays coupled with a focus on the measurement of the different complexes individually may enable us to measure such a gradient in the future.

Our histological analysis of both acutely administered exogenous adiponectin as well as steady-state endogenous levels have revealed several interesting observations. In all the organs investigated, adiponectin can be visualized in larger blood vessels. This is especially the case for visualization of endogenous adiponectin whose steady-state distribution is a reflection of adiponectin at various stages of degradation. In contrast, our pulsed administration of recombinant adiponectin allows us to follow a much more homogenous population. The staining of the vessels is consistent with a possible role of the adiponectin-binding protein T-cadherin (8). The lack of an intracellular signaling motif makes this protein an unlikely candidate as a signal transducer. Instead, T-cadherin may function to tether adiponectin to the vessel wall where a possible reductase may cleave the full-length adiponectin into the trimer. Accessibility to the hepatocytes is increased with the cysteine 39 mutant, suggesting that this 90-kDa complex may have more efficient access across the endothelium and the sinusoidal fenestrae as opposed to the wild-type protein that can be as big as 500 kDa to 1 megadalton. We have not addressed the question whether the published adiponectin receptors adipoR1 and adipoR2 are critically involved in this process.

It is also interesting to note that we detect a significant amount of signal in the kidney where it is primarily in the tubules. Whether clearance in the kidney is a phenomenon that is also relevant for native adiponectin or whether it is a secondary site that clears a liver-derived degradation product is not clear. However, an important role of the kidneys for adiponectin levels has been reported in several cases in patients with chronic kidney disease (19).

It remains intriguing that an abundant plasma protein such as adiponectin is cleared at such a rapid rate. This results in a very high biosynthetic rate in the adipocytes. Despite a high level of production and rapid clearance, it is surprising that the steady-state levels in circulation are remarkably stable and fluctuate with minimal diurnal variability. This implies that a communication axis between the different adipocytes, as well as among the different adipose pads, must be strictly maintained. Furthermore, plasma adiponectin is extremely stable, since it can be stored for 36 h without any significant losses due to degradation, suggesting that clearance-based mechanisms are the predominant method of elimination rather than degradation in plasma (20).

In summary, we have shown here for the first time the clearance rate for the key metabolic hormone adiponectin. We have furthermore shown that the clearance varies for the different isoforms of adiponectin, with HMW being cleared the slowest and the trimer the fastest. Finally, we demonstrate that the liver is the main site of clearance and the kidney only excretes final degradation products.

ACKNOWLEDGMENTS

This work was supported by National Institutes of Health Grants R01-DK55758 and R01-CA112023. N.H. is funded by a grant from University of Copenhagen. T.S. was supported by a postdoctoral fellowship from the American Heart Association (Heritage Foundation no. 0625998T).

No potential conflicts of interest relevant to this article were reported.

We thank members of the Scherer Laboratory for helpful comments and the UT Southwestern Live Cell Imaging Facility.

REFERENCES

1. Berg AH, Combs TP, Du X, Brownlee M, Scherer PE. The adipocyte-secreted protein Acrp30 enhances hepatic insulin action. Nat Med 2001;7:947–953
2. Kim JY, van de Wall E, Laplante M, Azzara A, Trujillo ME, Hofmann SM, Schraw T, Durand JL, Li H, Li G, Jelicks LA, Mehler MF, Hui DY, Deshaies Y, Shulman GI, Schwartz GJ, Scherer PE. Obesity-associated improvements in metabolic profile through expansion of adipose tissue. J Clin Invest 2007;117:2621–2637
3. Yamauchi T, Kamon J, Waki H, Terauchi Y, Kubota N, Hara K, Mori Y, Ide T, Murakami K, Tsuboyama-Kasaoka N, Ezaki O, Akanuma Y, Gavrilova O, Vinson C, Reitman ML, Kagechika H, Shudo K, Yoda M, Nakano Y, Tobe K, Nagai R, Kimura S, Tomita M, Froguel P, Kadowaki T. The fat-derived hormone adiponectin reverses insulin resistance associated with both lipoatrophy and obesity. Nat Med 2001;7:941–946
4. Hara K, Boutin P, Mori Y, Tobe K, Dina C, Yasuda K, Yamauchi T, Otabe S, Okada T, Eto K, Kadowaki H, Hagura R, Akanuma Y, Yazaki Y, Nagai R, Taniyama M, Matsubara K, Yoda M, Nakano Y, Tomita M, Kimura S, Ito C, Froguel P, Kadowaki T. Genetic variation in the gene encoding adiponectin is associated with an increased risk of type 2 diabetes in the Japanese population. Diabetes 2002;51:536–540
5. Yoon SJ, Lee HS, Lee SW, Yun JE, Kim SY, Cho ER, Lee SJ, Jee EJ, Lee HY, Park J, Kim HS, Jee SH. The association between adiponectin and diabetes in the Korean population. Metabolism 2008;57:853–857
6. Pajvani UB, Hawkins M, Combs TP, Rajala MW, Doebber T, Berger JP, Wagner JA, Wu M, Knopps A, Xiang AH, Utzschneider KM, Kahn SE, Olefsky JM, Buchanan TA, Scherer PE. Complex distribution, not absolute amount of adiponectin, correlates with thiazolidinedione-mediated improvement in insulin sensitivity. J Biol Chem 2004;279:12152–12162
7. Pajvani UB, Du X, Combs TP, Berg AH, Rajala MW, Schulthess T, Engel J, Brownlee M, Scherer PE. Structure-function studies of the adipocyte-secreted hormone Acrp30/adiponectin. Implications fpr metabolic regulation and bioactivity. J Biol Chem 2003;278:9073–9085
8. Hug C, Wang J, Ahmad NS, Bogan JS, Tsao TS, Lodish HF. T-cadherin is a receptor for hexameric and high-molecular-weight forms of Acrp30/adiponectin. Proc Natl Acad Sci U S A 2004;101:10308–10313
9. Yamauchi T, Kamon J, Ito Y, Tsuchida A, Yokomizo T, Kita S, Sugiyama T, Miyagishi M, Hara K, Tsunoda M, Murakami K, Ohteki T, Uchida S, Takekawa S, Waki H, Tsuno NH, Shibata Y, Terauchi Y, Froguel P, Tobe K, Koyasu S, Taira K, Kitamura T, Shimizu T, Nagai R, Kadowaki T. Cloning of adiponectin receptors that mediate antidiabetic metabolic effects. Nature 2003;423:762–769
10. Bjursell M, Ahnmark A, Bohlooly YM, William-Olsson L, Rhedin M, Peng XR, Ploj K, Gerdin AK, Arnerup G, Elmgren A, Berg AL, Oscarsson J, Linden D. Opposing effects of adiponectin receptors 1 and 2 on energy metabolism. Diabetes 2007;56:583–593
11. Liu Y, Michael MD, Kash S, Bensch WR, Monia BP, Murray SF, Otto KA, Syed SK, Bhanot S, Sloop KW, Sullivan JM, Reifel-Miller A. Deficiency of adiponectin receptor 2 reduces diet-induced insulin resistance but promotes type 2 diabetes. Endocrinology 2007;148:683–692
12. Schraw T, Wang ZV, Halberg N, Hawkins M, Scherer PE. Plasma adiponec-

tin complexes have distinct biochemical characteristics. Endocrinology 2008;149:2270–2282
13. Combs TP, Berg AH, Rajala MW, Klebanov S, Iyengar P, Jimenez-Chillaron JC, Patti ME, Klein SL, Weinstein RS, Scherer PE. Sexual differentiation, pregnancy, calorie restriction, and aging affect the adipocyte-specific secretory protein adiponectin. Diabetes 2003;52:268–276
14. Haluzik M, Colombo C, Gavrilova O, Chua S, Wolf N, Chen M, Stannard B, Dietz KR, Le Roith D, Reitman ML. Genetic background (C57BL/6J versus FVB/N) strongly influences the severity of diabetes and insulin resistance in ob/ob mice. Endocrinology 2004;145:3258–3264
15. Berg AH, Lin Y, Lisanti MP, Scherer PE. Adipocyte differentiation induces dynamic changes in NF-kappaB expression and activity. Am J Physiol Endocrinol Metab 2004;287:E1178–E1188
16. Combs TP, Wagner JA, Berger J, Doebber T, Wang WJ, Zhang BB, Tanen M, Berg AH, O'Rahilly S, Savage DB, Chatterjee K, Weiss S, Larson PJ, Gottesdiener KM, Gertz BJ, Charron MJ, Scherer PE, Moller DE. Induction of adipocyte complement-related protein of 30 kilodaltons by PPARgamma agonists: a potential mechanism of insulin sensitization. Endocrinology 2002;143:998–1007
17. Wolf AM, Wolf D, Avila MA, Moschen AR, Berasain C, Enrich B, Rumpold H, Tilg H. Up-regulation of the anti-inflammatory adipokine adiponectin in acute liver failure in mice. J Hepatol 2006;44:537–543
18. Valera Mora ME, Scarfone A, Calvani M, Greco AV, Mingrone G. Insulin clearance in obesity. J Am Coll Nutr 2003;22:487–493
19. Axelsson J, Stenvinkel P. Role of fat mass and adipokines in chronic kidney disease. Curr Opin Nephrol Hypertens 2008;17:25–31
20. Pischon T, Hotamisligil GS, Rimm EB. Adiponectin: stability in plasma over 36 hours and within-person variation over 1 year. Clin Chem 2003;49:650–652